Jurnal Pendidikan Fisika dan Keilmuan (JPFK)
Vol. 10, No.1., March 2024, pp. 56-80
P-ISSN: 2442-8868, E-ISSN: 2442-904X, DOI: http://doi.org/10.25273/jpfk.v10i1.19813

The Effect Of Annealing Temperature On The Properties Of Thin Zno Films Deposited Using Microwave-Assisted Spray Pyrolysis System

Nafiusokhib[1]*, Putut Marwoto[1], Sulhadi[1], Budi Astuti[1], Sugianto[1], Teguh Darsono[1], Siti Wahyuni[1], Alvin Fachrully Septiano[2]

[1] Departmen of Physics, Faculty of Mathematics and Natural Sciences,
Universitas Negeri Semarang
[2] Departmen of Radiodiagnostic Techniques and Radiotherapy STIKES An Nasher Cirebon, Indonesia.

e-mail: [1]nafiussohib@students.unnes.ac.id
*** Corresponding Author**

Abstract

This research aims to determine the optimal annealing temperature for the production of ZnO thin films using the microwave-assisted spray pyrolysis method. In the ZnO growth process, a high microwave temperature was used, with a spray pressure of 20 kg/m2, a nozzle distance of 12 cm, 3 layers, a spray duration of 5 seconds, and a 1-minute interval between layers. Annealing temperature variations included 300°C, 350°C, 400°C, 450°C, 500°C, 550°C, and 600°C. SEM results indicated that the best morphology was achieved at 400°C, with the smoothest and least cracked surface. EDX results showed the highest ZnO composition percentage at 450°C, which was 93.61%.The optical properties obtained from UV-Vis spectroscopy revealed the lowest absorption in the visible light wavelength range (400-700 nm) at an annealing temperature of 450°C. Furthermore, the highest transmittance and the lowest bandgap were observed at an annealing temperature of 450°C, measuring 90.77% and 3.00 eV, respectively. Crystal property analysis from XRD data revealed that all samples had a hexagonal wurtzite structure. The best crystal index was achieved at 450°C, with a value of 81.899%. Increasing the annealing temperature improved the crystal properties, as evidenced by a decreasing full width half maximum (FWHM) until 450°C, which was 0.476°.

Keywords: Annealing; Thin film; Microwave-assisted spray pyrolysis; ZnO

How to Cite: Nafiusokhib, N., Marwoto, P., Sulhadi, Astuti, B., Sugianto, Darsono, T., Wahyuni, S., & Alfin F.S. (2024). The Effect of Annealing Temperature on The Properties of Thin Zno Films Deposited Using Microwave-Assisted Spray Pyrolysis System. *Jurnal Pendidikan Fisika dan Keilmuan (JPFK)*, 10(1), 56-80. doi:http://doi.org/10.25273/jpfk.v10i1.19813

INTRODUCTION

Currently, the use of solar panels is increasing. This is due to the growing preference for environmentally friendly energy sources over fossil fuels. The high cost of solar cells can be reduced by using dye-sensitized solar cells (DSSC), making them more affordable (Hardani et al., 2016). DSSCs are known for their high efficiency. DSSCs based on 2% aluminum-doped ZnO nanorods can increase efficiency by 0.479% compared to pure ZnO (Iwantono et al., 2016) .DSSCs have the ability to absorb a broader spectrum compared to silicon-based solar cells, thanks to dyes that can extend the absorption spectrum from ultraviolet to visible light (Hardani et al., 2016). The main components of DSSCs are the working electrode, counter electrode, and electrolyte solution, which use transparent conductive oxide (TCO) glass. Besides being essential

for solar cells, TCO is used in various other applications such as displays, smart windows, touchscreens, light-emitting diodes (LEDs), and more (Rinaldi et al., 2016).

An ideal TCO material should have low resistivity, less than 10^{-3} Ωcm, and high transmittance, over 80% (Ponja et al., 2020). The ideal TCO should have high transparency over a wide spectrum, high electron carrier mobility, and good stability in different environments (Zhou et al., 2014). TCO is typically made from compounds that involve two or three metal-bound elements (Afre et al., 2018). One suitable material for TCO candidates is metal oxide semiconductors (MOS) because they are metal oxide semiconductors composed of metal ions and oxygen (Samad et al., 2020). Materials such as zinc oxide (ZnO), titanium dioxide (TiO_2), tin oxide (SnO_2), silicon dioxide (SiO_2), zirconium dioxide (ZrO_2), among others, are part of the MOS group (Wijesinghe et al., 2019). Currently, the most commonly used TCO materials are Indium Tin Oxide (ITO) and Fluorine Tin Oxide (FTO) due to their excellent optical and electrical properties (Zheng et al., 2014). However, these materials have limitations, including the rising cost of indium, inability to be processed at high temperatures, and low flexibility, which has led to the search for alternative materials like ZnO (Zheng et al., 2014).

Zinc oxide (ZnO) has emerged as a promising TCO alternative due to its attractive properties, including a wide bandgap of approximately 3.37 eV, high electron mobility, large surface area, and the ability to grow at relatively low temperatures around 200-400°C (Loureiro et al., 2014). When in the form of a thin film, ZnO exhibits high transmittance, approximately 90%, in the visible light range (Tian et al., 2016). This makes ZnO a valuable material for photocatalysis and photoanodes in DSSCs. The Food and Drug Administration (FDA) has classified ZnO as a safe compound, making it suitable for various applications (Espitia et al., 2016). ZnO is often used as a photoanode in DSSCs to replace TiO2 due to similar electron transfer processes, high electron mobility, and cost-effectiveness (Vittal & Ho, 2017).

There are various methods for producing ZnO thin films, such as sol-gel, sputtering, hydrothermal, pulsed laser deposition, spray pyrolysis, and plasma-enhanced chemical vapor deposition (PECVD). Each method has its advantages and disadvantages. Spray deposition offers benefits like high deposition rates, ease of use for various materials, and environmental friendliness due to minimal hazardous waste (Rustandi et al., 2012). Spray pyrolysis, in particular, provides cost-effective operation, requires minimal precursor, and operates under ambient pressure(Saha et al., 2020). However, it still faces challenges like difficulties in controlling crystal growth temperature and achieving accurate control, which can be addressed with proper equipment like microwave heating (Zhang et al., 2017).

To obtain the best results in ZnO synthesis using the microwave-assisted spray pyrolysis method, several factors need to be considered, including heating temperature, heating time, distance between the substrate and the spray nozzle, microwave power, spray pressure, solution synthesis techniques, and annealing temperature. An earlier study found that the optimal conditions were a maximum degree of heating (250°C), heating time (30 minutes), and a distance between the substrate and the spray gun nozzle (12 cm) for TCO synthesis (Nafisah, 2022). Further research needs to explore other parameter variations to optimize the results. Additionally, to achieve desirable film properties, the appropriate annealing temperature must be employed (Darsono et al., 2021). Annealing at high temperatures enhances film thickness and alters particle

size and shape (López-Suárez et al., 2020). Proper annealing temperature allows solvents in the thin film to evaporate, reducing hardness and improving mechanical properties (Mahmudah, 2016). The optimal annealing temperature can also affect crystal orientation and improve crystalline properties (Sugianto et al., 2016). It is essential to control the deposition conditions and annealing treatment to achieve the desired film properties (Kurtaran, 2021). Based on this background, research on the most appropriate annealing temperature for the production of ZnO thin films using the microwave-assisted spray pyrolysis method has been conducted.

METHODS

Time and Place of Research

The research was conducted in the Material Physics Laboratory of the Department of Physics, Faculty of Mathematics and Natural Sciences, Universitas Negeri Semarang. This research was carried out from January to March 2023.

Equipment and Materials

The equipment used includes a commercial microwave oven type Sharp R-21D0 (S) – IN- 450 W, a spray gun, furnace, hotplate, magnetic stirrer, spatula, tweezers, petri dishes, digital scales, rulers, glass cutters, ultrasonic baths, measuring glasses, and glass beakers. Characterization equipment used includes Scanning Electron Microscopy (SEM), X-Ray Diffraction (XRD), UV-Vis Spectrophotometer, and Energy Dispersive X-Ray (EDX). The data obtained were then analyzed using a laptop and software such as MatLab and Origin.

The materials used include Zinc Acetate Dihydrate ($Zn(CH_3COO)_2.2H_2O$) 99.9% as a precursor, methanol 99.9% as a solvent. Other materials include isopropanol, ethanolamine, acetone 99%, and deionized water (aquades) for substrate cleaning, as well as compressed nitrogen gas and glass slides.

Preparation of Materials

The substrate used is glass slides. Before use, the glass slides were cut into squares measuring 1 x 1 cm and cleaned of dust and contaminants adhering to the surface. The substrate was cleaned using acetone, methanol, and deionized water in an ultrasonic bath for 15 minutes at each stage. Once cleaned, the substrate was dried by blowing nitrogen gas over the entire surface to speed up the drying process and remove any remaining dust.

Deposition Using the Microwave Assisted Spray Pyrolysis Method

The microwave-assisted spray pyrolysis system is depicted as shown in Figure 3.2. The commercial microwave used operates at a frequency of 2.45 GHz, typically used for heating food. The spray gun was appropriately positioned on the top cavity wall of the microwave, creating holes through which the precursor

solution was sprayed, generating plasma when the power was turned on. The plasma formed will be deposited onto the glass substrate.

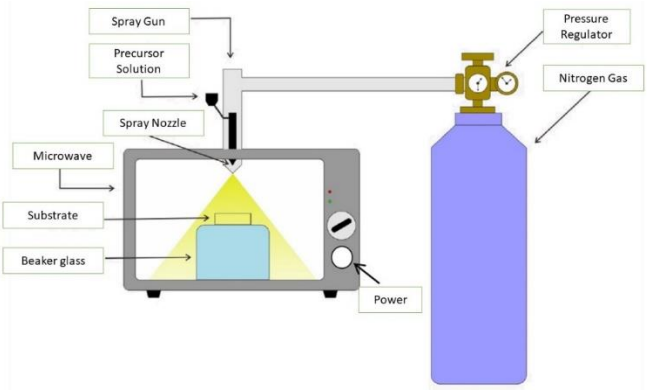

Figure 1. Microwave Assisted Spray Pyrolysis System Configuration

The ZnO solution is synthesized by mixing 2.195 g of zinc acetate dihydrate with 20 mL of isopropanol in a beaker glass. Mixing of the materials is done on a hotplate stirrer at a stirring speed of 1000 rpm at room temperature for 10 minutes. Once the mixture is thoroughly mixed and forms a clear solution, the hotplate temperature is raised to 70°C, and the beaker glass is covered with aluminum foil. When the temperature is raised, 1.452 mL of methanolamine is added to the solution. This mixing process is carried out for 1 hour until a homogeneous and stable solution is obtained without any sediment. The solution is then allowed to sit for 24 hours before the deposition process on the substrate.

The substrate is heated on a hotplate to a temperature of 250°C and placed in the microwave with the highest temperature setting, with a duration of 30 minutes. After 10 minutes of heating, the substrate is sprayed with the ZnO solution by spraying it for 5 seconds with 3 layers, and each layer is given a 1-minute interval. The substrate, which has been coated with the ZnO solution, is left in the microwave for 20 minutes.

Annealing

In this research, annealing is performed by heating the thin film in a furnace after ZnO is deposited in the microwave. The annealing temperature used in this research varies from 300, 350, 400, 450, 500, 550, and 600°C. The first step of the annealing process is to set the furnace temperature to 300°C for 1 hour. The calculation of time starts after the furnace temperature stabilizes at 300°C. After waiting for 1 hour, the furnace temperature is gradually lowered to 100°C, with each lowering step waiting for the temperature to stabilize for 5 minutes. The sample can then be removed when the furnace has returned to room temperature. This process is also repeated for temperatures of 350-600°C.

Sample Characterization

The synthesized samples are then characterized to determine morphology, elemental composition, crystal structure, and optical properties. SEM-EDX analysis is performed to determine the morphology and elemental content of the samples, XRD analysis is carried out to determine crystal structure, and UV-Vis analysis is used to obtain data on absorbance, transmittance, and bandgap. The transmittance value can be obtained by comparing the light intensity after passing through the material to the light intensity before passing through, expressed as a percentage (Bizarro et al., 2011), as seen in Equation (1):

$$T = \frac{I}{I_0} 100\% \quad (1)$$

Here, T represents the transmittance value of the material (%), and the ratio of light intensity after and before passing through the material can be obtained from Equation (2):

$$\frac{I}{I_0} = e^{-\alpha b} \quad (2)$$

Where b is the thickness of the formed film, and α is the absorption coefficient. The absorption coefficient (α) can be determined using Equation (3):

$$\alpha = -\frac{1}{b} lnT \quad (3)$$

To determine the energy of photons in light emitted to the material at a specific wavelength, it is expressed in Equation (4):

$$E = hv = \frac{hc}{\lambda} \quad (4)$$

Here, E represents the energy of a photon (Joules), λ is the wavelength of light (meters), c is the speed of light in a vacuum (3 x 10^8 m/s), and h is Planck's constant (6.62 x 10^{-34} Js).

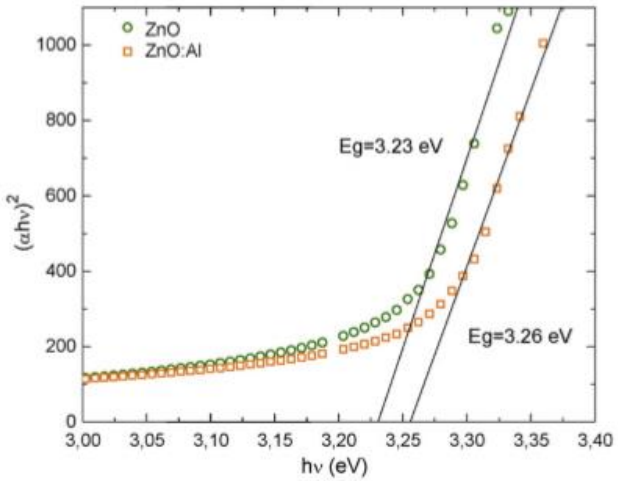

Figure 2. Graph determining the energy bandgap using the Tauc Plot method

The energy bandgap of a semiconductor material is determined through the Tauc Plot method by plotting (αhv)² on the ordinate against Eg and hv on the abscissa, and then drawing a trendline on the graph as shown in Figure 3.3.

Based on this graph, the relationship between α and hv for the energy bandgap of semiconductor materials is established. To determine the ordinate value in Figure 1, it is indicated in Equation (5):

$$(\alpha hv)^2 = A(hv - Eg) \tag{5}$$

Where α is the absorption coefficient, Eg is the energy of the photon, and A is a constant related to the energy bandgap properties.

XRD is used to identify the crystal structure of a solid substance by comparing the d-spacing values and peak intensities with standard data. X-rays are electromagnetic radiation with wavelengths (λ) ranging from 10 nm to 100 pm, typically generated by bombarding high-energy electrons onto a metal target. X-rays have high penetration, allowing them to reveal the periodicity of crystals. By using the Debye-Scherrer formula:

$$D_{hkl} = \frac{0.9\lambda}{\beta \cos\theta} \tag{6}$$

D_{hkl} (the average crystal size) can be obtained from the XRD data analysis. Here, λ is the X-ray wavelength, θ is the diffraction angle, and β is the Full Width at Half Maximum (FWHM). During the analysis, Bragg's law is also used to determine the lattice interplanar spacing of nearby crystal planes:

$$d = \frac{\lambda}{2 \sin\theta} \tag{7}$$

Where d is the lattice interplanar spacing, θ is the diffraction angle, and λ is the X-ray wavelength.

Furthermore, FWHM data from XRD can be used to find strain (ε), stress (σ), and crystal dislocation (δ) using the following formulas:

$$\varepsilon = \frac{\beta}{4\tan\theta} \quad (8)$$

$$\sigma = -233\varepsilon \ \ (GPa) \quad (9)$$

$$\delta = \frac{1}{D^2} \quad (10)$$

Here, ε represents crystal strain, β is the FWHM value, θ is the diffraction angle, σ is the thin film pressure, and D is the average crystal size.

When a material is exposed to X-rays, the transmitted beam's intensity is lower than the incident beam's intensity. This is due to the material's absorption and scattering by its atoms. The scattered X-ray beams can either cancel each other out due to phase differences or reinforce each other because of similar phases. The X-ray beams that reinforce each other are referred to as diffracted beams (Yousaf et al., 2021).XRD data can be used to determine the crystallographic index of a material. The crystallographic index can be calculated using the formula:

$$CI = \frac{I_c}{(I_c + I_a)}\ 100\% \quad (11)$$

Here, CI is the crystallographic index, I_c is the crystal's intensity, and I_a is the amorphous intensity (Lin et al., 2019).

RESULTS AND DISCUSSION (70%)

Results of ZnO Thin Film Deposition

In this research, a deposition of ZnO thin films was carried out using the microwave-assisted spray pyrolysis method. The ZnO precursor was prepared using the sol-gel method with $Zn(CH_3COO)_2.2H_2O$ and isopropanol as the solvent. Isopropanol was chosen as the solvent because it readily evaporates, ensuring that when it is sprayed onto the substrate, the solution evaporates, leaving behind the ZnO. The spraying process was conducted at a distance of 12 cm, which was determined to be the optimal distance for spraying with a pressure of 20 kg/cm^2. The thin film coating was applied three times, following the procedure used by Nafisah (Nafisah, 2022), who obtained the best results with this coating.

This research included variations in annealing temperatures from 300°C to 600°C with a 50°C interval, each for a duration of 1 hour. Variations in annealing were performed because annealing can influence the optical properties (Lim et al., 2017), crystal structure (Sugianto et al., 2016), and electrical resistivity of a material (Anitha et al., 2019). The impact of annealing temperature on the properties of ZnO thin films in the microwave-assisted spray pyrolysis method was investigated through sample characterization.

The synthesized samples were subsequently characterized to determine their morphology, elemental composition, crystal structure, and optical properties. SEM-EDX analysis was performed to investigate the morphology and elemental composition of the samples. XRD analysis was carried out to understand the crystal structure, and UV-Vis testing was performed to obtain data on absorbance, transmittance, and bandgap properties. The initial characterization in the synthesis of thin films involves a CCD microscope, as shown in Figure 3.

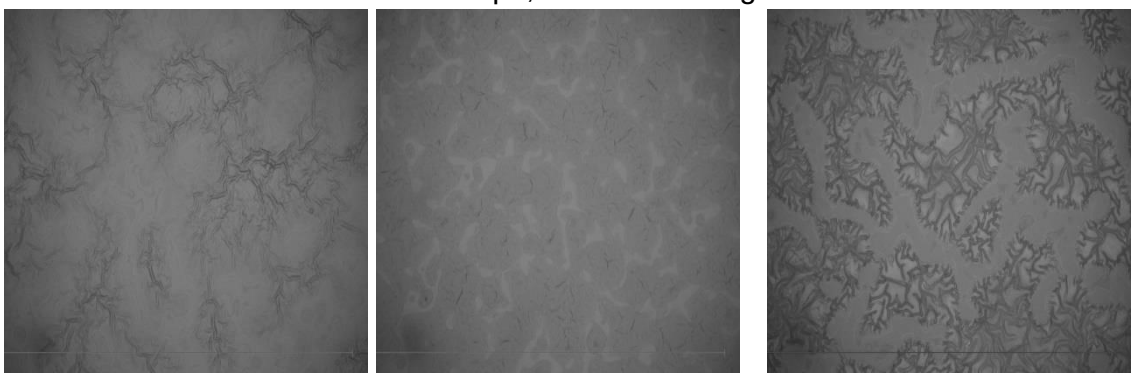

a.300 ^{o}C b.350 ^{o}C c.400 ^{o}C

d.450 ^{o}C e.500 ^{o}C f.550 ^{o}C

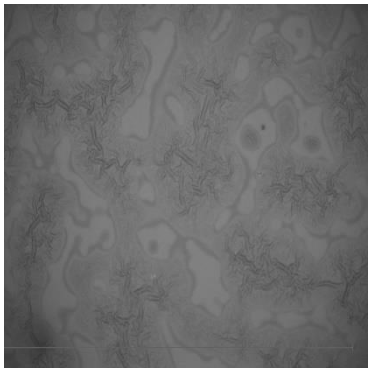

g.600 ^{o}C

Figure 3. CCD Results at 1000x magnification with annealing temperature variations (a) 300°C, (b) 350°C, (c) 400°C, (d) 450°C, (e) 500°C, (f) 550°C, and (g) 600°C.

The CCD results are used to confirm the presence of the ZnO thin film on the substrate. Based on the CCD microscope results in Figure 3, it is evident that the thin film has formed on the substrate, as indicated by the appearance of spots corresponding to thin film growth. All 7 annealing variations exhibit different surface characteristics due to the different annealing temperatures applied to each sample. Samples annealed at 300°C, 350°C, and 600°C show signs of ZnO thin film growth, although it is not as pronounced as in samples annealed between 400°C and 550°C. This is because atoms released from the target move randomly, resulting in irregular arrangements on the substrate surface (Hadi et al., 2013). The sample annealed at 550°C displays more noticeable cracks compared to the others. Further analysis to understand the properties of the ZnO thin film is conducted through additional characterization.

Characterization Results of the ZnO Thin Film

Composition and Morphological Properties

Thin films deposited using annealing variations from 300°C to 600°C with a 50°C range have differences in their morphology. In Figure 4, it can be observed that the surface of the ZnO thin film deposited using microwave-assisted spray pyrolysis at an annealing temperature of 300°C has a relatively rough distribution, and no crack holes are found in any part. At an annealing temperature of 350°C, the morphological structure begins to improve and appears smoother compared to the surface at 300°C, but some folds are visible. Temperatures below 400°C, such as 300°C and 350°C, result in a rough surface with folds because the lower temperature causes a longer evaporation of the ZnO precursor in the film layer due to slower reaction kinetics.

The thin films deposited using annealing variations from 300°C to 600°C with a 50°C range exhibited differences in their morphology. In Figure 4, the surface of the ZnO thin film deposited using microwave-assisted spray pyrolysis at an annealing temperature of 300°C appears to have a relatively rough distribution

with no observable cracks or folds across the surface. At an annealing temperature of 350°C, the morphological structure starts to improve and appears smoother compared to the surface at 300°C, though some folds are still noticeable. Annealing at temperatures below 400°C, specifically 300°C and 350°C, resulted in rougher surfaces and folds due to the longer evaporation of the ZnO precursor in the film layer caused by slower reaction kinetics.

Sample annealed at 400°C showed the smoothest surface structure compared to the other samples, with no cracks or folds visible. Samples with annealing variations at 450°C exhibited a rougher surface structure than the 400°C sample but were smoother compared to the 300°C and 350°C samples. Cracks were also observed in the 450°C sample, though they were relatively minimal compared to the samples annealed at 500°C and 600°C. The surface structure at 500°C appeared smoother than at 450°C, but more cracks were observed. Samples annealed at 500°C also started to exhibit folds. At 500°C, the film experienced cracking and folding, as the temperature exceeded the optimum temperature for crystal growth in ZnO. Annealing at temperatures between 400°C and 500°C resulted in improved morphological characteristics because the higher heating rate caused the precursor ZnO to evaporate more quickly into the external environment, which led to changes in the solid structure of the substrate and improved morphological appearance.

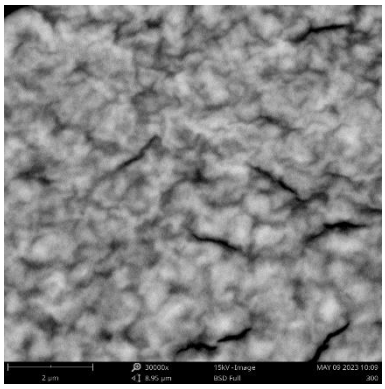

a.300^{o}C

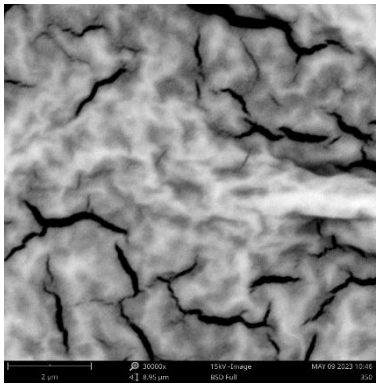

b.350^{o}C

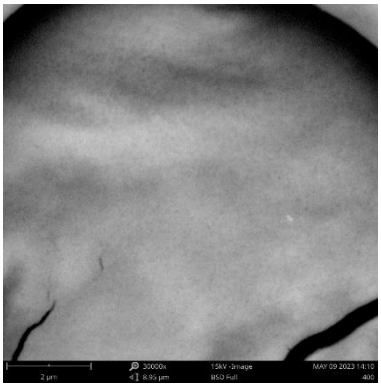

c.400^{o}C

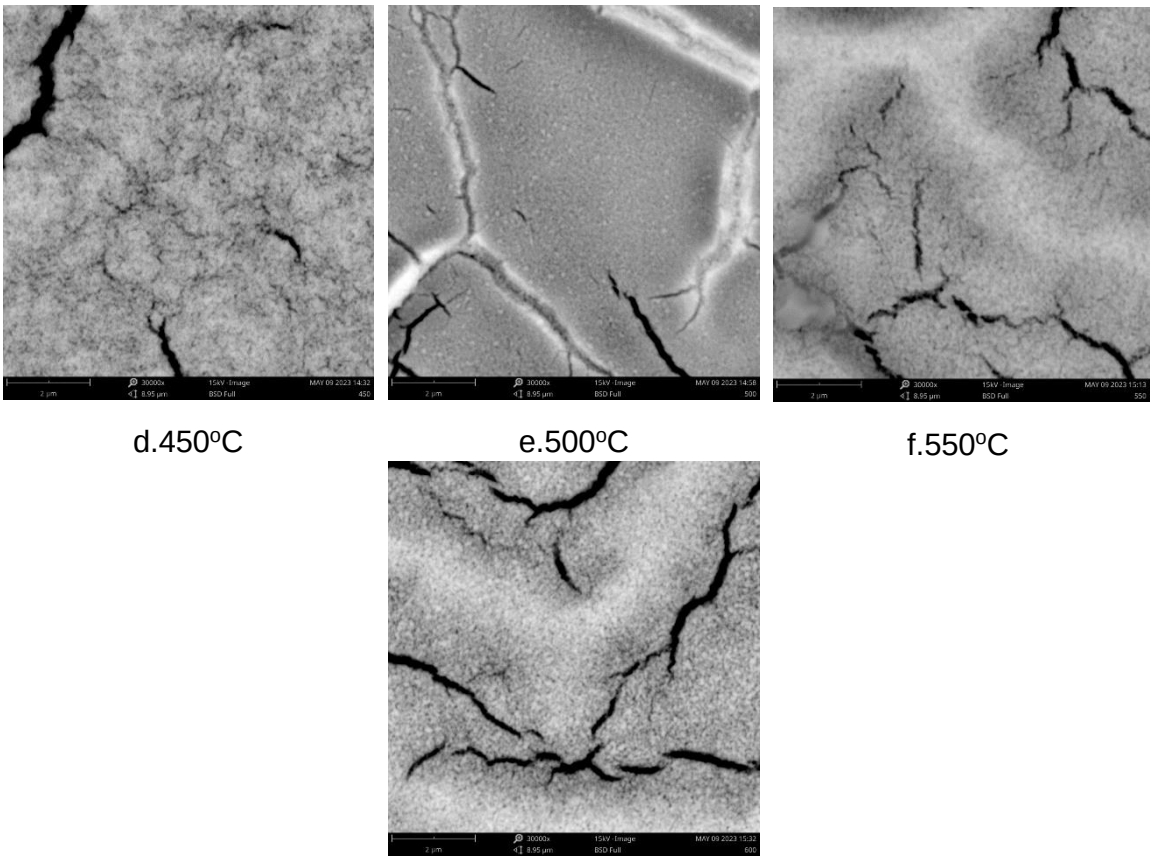

d.450ºC e.500ºC f.550ºC

g.600ºC

Figure 4. SEM Results of ZnO Annealing at 30,000x Magnification

At 550°C, the surface started to appear rougher again, with more cracks and clearer folds compared to 500°C. In the samples subjected to annealing at 600°C, cracks, roughness, and folds were most prevalent and clearly visible compared to the other samples. Annealing at 550°C and 600°C resulted in less favorable outcomes due to the increased heat temperature surpassing the substrate's ideal heat, which then hindered some of the ZnO precursor on the substrate from increasing the evaporation rate at higher temperatures. In this case, the competition between the film expansion kinetics and heat convection, as well as evaporation at different temperatures, led to variations in the thickness of the deposited film, ultimately affecting the thin film's morphology.

Table 1. EDX Results: Concentrations of Zn, O, ZnO, and Si

Temperature (ºC)	Concentration Amount			Concentration amount
	Zn (%wt)	O(%wt)	Si(%wt)	ZnO(%wt)
300	66.42	24.30	9.28	89,91

Temperature (°C)	Concentration Amount			Concentration amount ZnO(%wt)
	Zn (%wt)	O(%wt)	Si(%wt)	
350	71,09	21,95	6,95	92,72
400	71.76	20.62	4.89	92,13
450	71,26	22,68	6,06	93,61
500	78.93	14.22	6.85	93.48
550	70.29	22.62	7.09	92.51
600	70.09	22.17	7.74	91.85

Annealing treatments serve to enhance the morphological properties of thin films by providing thermal energy to the electrons, causing them to move from an unstable state to a stable one by occupying the empty spaces within the crystal lattice of the ZnO thin film. The optimum annealing temperature will relax the stress or strain of the thin film due to the differences in thermal coefficients between the substrate and the ZnO precursor during deposition. The presence of non-smooth sample surfaces is attributed to the non-uniform particle size (Darsono et al., 2021). The presence of bends and folds in the thin film is due to the diffusion of smaller ZnO grain atoms that form larger grains, resulting in the reduction of grain boundaries. Uniform and compact crystallite size distribution that covers the substrate without cracks and appears smooth is evident in Figure 4. at an annealing variation temperature of 400°C. Cracks that appear in thin films are a result of the film's very low thickness. Thin film thickness influences the morphological structure of the thin film; the thicker a thin film, the rougher its surface appears compared to the 500°C sample. Thin films subjected to excessive thermal energy beyond the optimal temperature will develop cracks as the electrons move from their stable conditions (Jun et al., 2012).

The results of the observations indicate that the sol-gel solution synthesis technique and annealing variation for ZnO thin films significantly impact changes in morphological structure. Based on Figure 4., this study's results are in line with Zhang et al (Zhang et al., 2017), where increasing the annealing temperature makes the surface smoother up to 500°C. At 450°C, the surface is still rough due to the film's thickness, as the deposition took slightly longer. The increase in cracks corresponds to the rise in annealing temperature. From the SEM results, it is evident that the best sample is within the 400°C annealing temperature range, as shown by its smoother surface structure with minimal cracks. Table 1 shows the

concentration amounts of Zn, O, and ZnO in the various annealing samples obtained from EDX. The EDX data for the ZnO thin films indicate that the highest concentration of Zn and the lowest concentration of O_2 are found in samples annealed at temperatures ranging from 400°C to 500°C.

This is related to the morphology observed in SEM characterization. Based on the morphological results at temperatures between 400°C and 500°C, the surfaces are the smoothest, with few cracks and no folding compared to the other samples. These results align with the research conducted by Marwoto et al.(Marwoto et al., 2019), where low oxygen content in thin films can indicate oxygen vacancies within the crystal structure. Conversely, an excess of oxygen can lead to defects in the film, resulting in a decrease in crystal quality. The higher Zn content improves the conductivity of the thin film due to its metallic properties.

Optical Properties

The optical properties observed in the ZnO thin films are determined through characterization using UV-Vis in the wavelength range of 300-800 nm. Wavelengths below 300 nm are excluded as they suffer from noise due to air interference. This testing was conducted in the Unnes Physics lab. Light from the deuterium lamp in the UV-Vis, which is polychromatic in nature, is transformed into monochromatic light. A light beam of a specific wavelength is passed through samples containing certain substances. The light passing through these substances yields information on transmittance, absorption, and band gap energy. Polychromatic light that hits a substance is absorbed at specific wavelengths because there are valence electrons within a molecule that play a role in forming a material.

Based on the UV-Vis data in Figure 5., it can be seen that at a wavelength of 300 nm, ZnO thin film deposition at annealing temperatures between 300°C and 600°C results in a maximum absorbance of 4 au. The absorbance in the samples appears to decrease as the wavelength increases. Differences are noted at a wavelength of 350 nm and beyond, which are wavelengths within the visible light spectrum frequently emitted by sunlight. These differences are attributed to the dependence of absorbance values on the film's morphology. Thicker morphologies of the thin film result in higher absorbance.

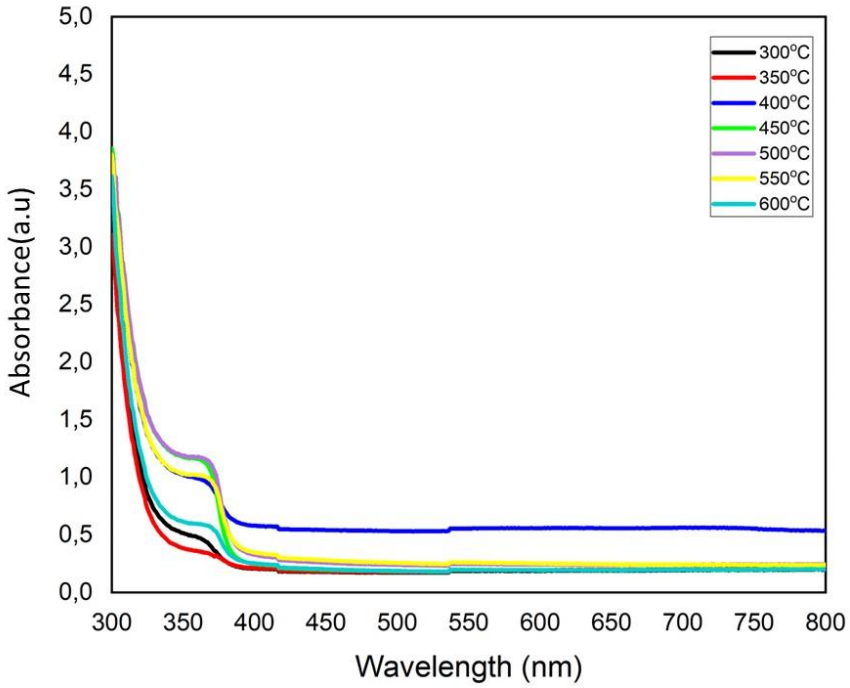

Figure 5. Absorbance of ZnO thin films with annealing variations (a) 300°C, (b) 350°C, (c) 400°C, (d) 450°C, (e) 500°C, (f) 550°C, and (g) 600°C

The absorbance values for all samples decrease with increasing wavelength. This is a characteristic of absorption in ZnO semiconductors. As shown in Figure 5., maximum absorbance occurs at wavelengths below 400 nm, indicating that all samples absorb infrared light. Beyond 400 nm, absorption continuously decreases, suggesting that very little visible and near-infrared light is absorbed, and more light is transmitted through the thin film (Astuti et al., 2020). A good TCO (transparent conductive oxide) is one that has low absorbance levels. Well-transmitted and unabsorbed light is the result of reflection by the thin film. Thicker layers with smoother surfaces cause light to be reflected (Saha et al., 2020). This also indicates that the more ZnO deposited in the film, the more light is absorbed. The absorption coefficient, which indicates the optical absorption of the thin film, can be used as a parameter to calculate the bandgap energy value. To determine the bandgap of the thin film, you can use the absorption coefficient and the photon energy passing through the thin film. The measurement of the bandgap energy of a semiconductor material is essential because the bandgap energy affects the electron transition properties with respect to photon frequency. The bandgap energy of the ZnO thin film is obtained through the processing of absorption data using the Tauc Plot method from Equation 9.

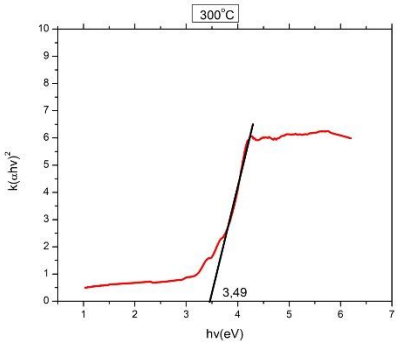

a.300ºC

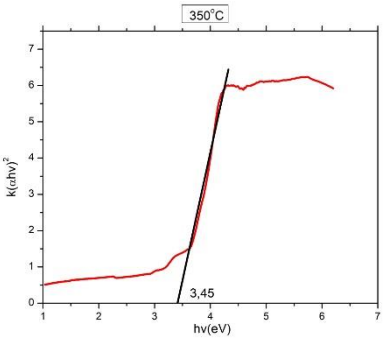

b.350ºC

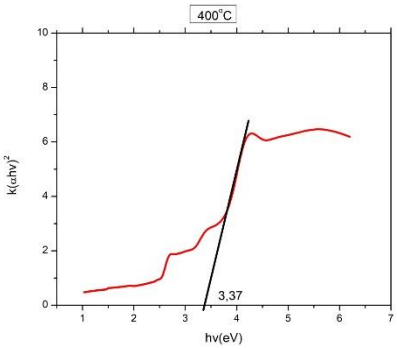

c.400ºC

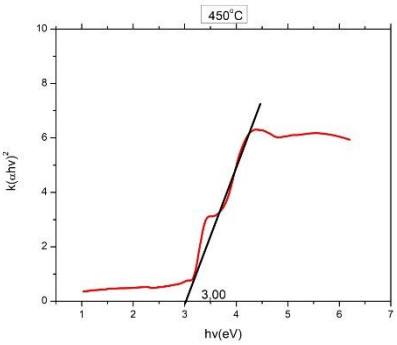

d.450ºC

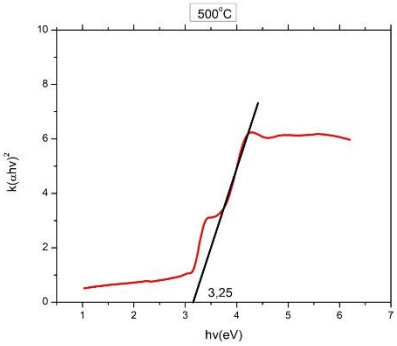

e.500ºC

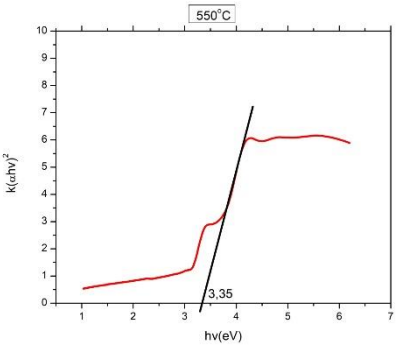

f.550ºC

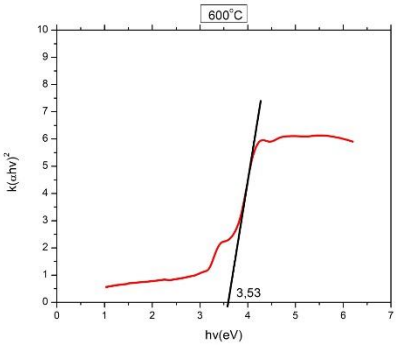

g.600ºC

Figure 6. Bandgap Graph of ZnO Thin Films

From this equation, a curve is generated showing the relationship between $(\alpha hf)^2$ and photon energy (Rashid et al., 2018). The linear line on the graph of this curve indicates the bandgap value, as shown in Figure 6, with the point where the graph intersects the horizontal axis indicating the bandgap energy width. Using equation 5, the bandgap energy values for each sample are obtained and summarized in Figure 6. From this data, it can be seen that the ZnO sample annealed at 300°C has a bandgap energy of 3.49 eV, and the bandgap energy decreases with each increase in annealing temperature up to 450°C. The bandgap value for the ZnO sample at 350°C is 3.45 eV, at 400°C it is 3.37 eV, and at 450°C it is 3.00 eV. Then, at 500°C, it increases again to 3.25 eV and continues to increase at 550°C and 600°C, with values of 3.35 eV and 3.53 eV, respectively.

These results indicate that the increase in annealing temperature causes atomic vibration, resulting in an increase in the atomic spacing. When the spacing between atoms increases, it leads to a decrease in the potential energy of electrons and the bandgap energy (Wypych, 2015). These findings are consistent with the research conducted by Aryanto et al.(Aryanto et al., 2020) and Sulhadi et al.(Sulhadi et al., 2021), which show that the increase in bandgap energy starts from a heating temperature of 450°C and decreases again at an annealing temperature of 600°C. A smaller bandgap in the thin film makes it easier to convert sunlight into electricity because a smaller bandgap requires less photon energy to move electrons from the valence band to the conduction band. Based on Figure 6, the samples that perform best in converting light into electricity are found in the annealing temperature variation of 450°C.

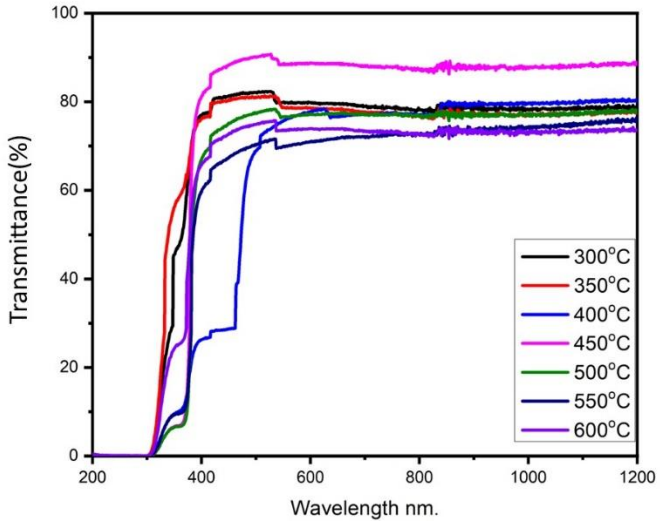

Figure 7. Graph of Transmittance Percentage vs. Wavelength

The transmittance of the thin film can be seen in Figure 6. Each sample has a different transmittance value. Figure 7 shows that the annealing temperature variations can influence the transmittance value of the thin film. In Figure 6, it is

evident that in visible light, many samples are highly transmissive. The maximum transmittance values achieved for each annealing temperature variation are shown in Table 2. The transmittance of ZnO thin films at the annealing temperature of 450°C is higher compared to the films annealed at other temperatures. The ZnO thin film annealed at 450°C exhibits relatively high transmittance, measuring 90.77%. Among all the synthesized samples, the lowest transmittance is observed in the sample annealed at 600°C, with a maximum transmittance of 75.77%.

Table 2. Maximum Transmittance for Each Temperature Variation

Temperature (°C)	Transmittance (%)
300	82,29
350	81,06
400	80,47
450	90,77
500	78,34
550	76,38
600	75,77

The transmission spectrum produced by a material is related to the quality of the resulting ZnO thin film crystal (Ashok et al., 2020). Low transmittance values are typically due to non-uniform and rough surfaces of the thin film, resulting in high light reflection and minimal transmission (Muchuweni et al., 2016). The high optical capabilities of thin films can be attributed to the annealing process. The bandgap expands due to the quantum size effect of the nanocrystalline structure in the thin film formed during annealing (Rashid et al., 2018). Thin films that have undergone annealing exhibit improved properties and quality compared to films without annealing (Sulhadi et al., 2015).

When atoms interact with each other, valence electrons in each atom will overlap and form bonds. Atoms with high electronegativity will form strong covalent bonds. If many strong covalent bonds are formed, the orbitals will form energy band gaps. Each material has a characteristic energy band gap that depends on the electronegativity of the constituent atoms and the type of bonding. The energy of light absorbed by the material also causes electron transitions between discrete energy levels and the conduction or valence bands (Celarel et al., 2018). The annealing temperature of thin films causes any remaining solvents to evaporate more quickly, leaving larger ZnO particles. This can lead to aggregation and an increase in the particle size of the film. When the particle size increases, grain boundary scattering decreases, which, in turn, can result in a decrease in transmittance or an increase in absorbance (Kasirajan et al., 2022).

A common requirement for thin films to be used as TCO (Transparent Conductive Oxide) is to have a transmittance of 70-90% in the visible light range (Sinaga, 2015). Another property of TCO is to have a minimum bandgap of 3.00 eV (Wang et al., 2013). Based on the bandgap size, all samples meet the requirements for application as TCO devices. However, the transmittance of the ZnO thin film at 600 °C annealing temperature only reached 75.77%. This is due to the large grain size and rough surface structure. Another factor is the transmission spectrum formed by a material, which is related to the crystal quality of the thin film.

Crystal Structure

The next property analyzed is the crystal structure, which is essential to understand because it relates to the electronic structure of ZnO thin films. The ZnO thin films successfully grown on glass substrates were characterized for their crystal properties using XRD (X-ray Diffraction). This characterization used a Cu radiation source with a wavelength of 1.540590 Å.

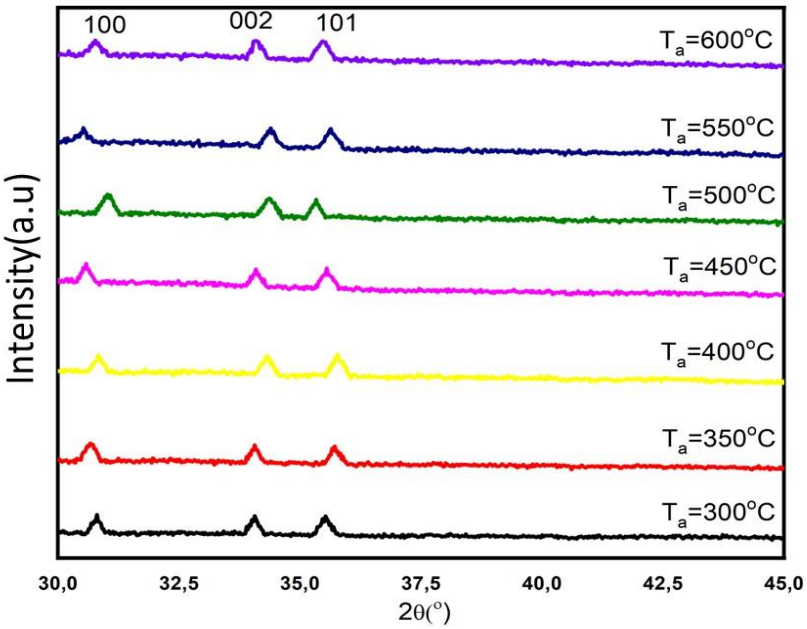

Figure 8. XRD Results Graph of ZnO Thin Films with Various Annealing Temperatures (Ta)

The XRD measurements for all samples are shown in Figure 8., indicating that the crystalline phase of ZnO is formed in nearly all samples, although the intensity appears to be low. The ZnO samples annealed at temperatures from 300°C to 600°C produce polycrystals with crystal plane orientations (100) at an angle of 30.5°, (002) at an angle of 34.0°, and (101) at an angle of 35.3°. These three crystal plane orientations signify that the ZnO thin films formed have a hexagonal wurtzite structure (JCPDS no 01-075-1526) (Abidah, 2022). From the XRD graph in Figure 8., it can be observed that the dominant crystal plane in the ZnO thin films annealed at temperatures between 300°C and 600°C is the (101) crystal plane. This suggests that the ZnO thin films grow parallel to the a and c axes on this crystal plane. This finding is consistent with the research conducted by Mehmood et al. (Mehmood et al., 2021), which identified the (101) crystal plane as the most dominant plane in ZnO. ZnO annealed at 350°C to 600°C undergoes a crystalline phase, with measurable crystal intensities exceeding 1000 counts per second. The presence of a crystalline phase and the low crystal intensity in ZnO at 300°C are due to the relatively low annealing temperature. Such a significantly lower annealing temperature than the optimum temperature hinders the film's growth (Reeja-Jayan et al., 2012).

The results of the XRD characterization also provide information on the values of crystal grain size (D), strain (ε), stress (σ), and crystal dislocations (δ), which can be calculated according to equations (6-10) summarized in Table 3. The XRD data processed using a matching technique indicates a hexagonal wurtzite crystal structure unit cell, with growth along the a and c crystal lattice parameters.

In Table 3., it can be seen that the full width at half-maximum (FWHM) tends to narrow as the crystal grain size increases, and the crystal stress decreases. This indicates that the smaller the FWHM, the more stable the crystal. The FWHM values for the ZnO thin film samples annealed at temperatures from 300°C to 600°C tend to decrease, from 0.547° to 0.513°. A smaller FWHM value suggests better crystal quality because smaller FWHM values indicate that atoms can bond more easily and are oriented more precisely.

The FWHM values obtained are then used to determine the crystal grain size (crystallite size). The crystallite size of ZnO annealed at temperatures from 300°C to 600°C ranges from 2.939 nm to 12.012 nm, with an average increase of 20%. This corresponds with the findings of Chaitra et al. (Chaitra et al., 2017), who noted that crystal size increases with higher annealing temperatures. Smaller particle sizes allow for more orderly atomic arrangements, reducing defects and distortions in the thin film's crystal structure. Fewer defects in the thin film can enhance its conductivity and optical quality.

The next parameter is crystal strain (ε), with an average value ranging from 0.028% to 0.037%, and stress (σ) ranging from 6.605 GPa to 8.609 GPa. The negative sign indicates that the crystal's residual stress is compressive (Gadallah & El-Nahass, 2013). Crystal stress is directly related to the atomic bonding energy between crystals (Marwoto et al., 2019), and lower σ values indicate greater crystal stability. Data indicates that the stress decreases from 8.609 GPa to 6.605 GPa as the annealing temperature increases from 300°C to 600°C. This is because higher annealing temperatures provide more room for atoms to move and align to create a perfect crystal structure, leading to a reduction in dislocation density.

Table 3. Crystal Plane (101) Parameters for Annealing Temperature Variations of 300°C to 600°C

Parameter	300 ^{o}C	350 ^{o}C	400 ^{o}C	450 ^{o}C	500 ^{o}C	550 ^{o}C	600 ^{o}C
Grid orientation (Å)	a = b = 5,21 c = 3,25	a = b = 5,21 c = 3,25	a = b = 5,21 c = 3,25	a = b = 5,21 c = 3,25	a = b = 5,21 c = 3,25	a = b = 5,21 c = 3,25	a = b = 5,21 c = 3,25
FWHM (^{o})	0,547	0,497	0,480	0,476	0,485	0,491	0,513
Crystal Index (%)	56,421	54,636	54,441	81,899	72,601	57,887	51,591
Crystal distance (nm)	3,473	3,671	3,022	3,653	3,686	3,366	3,347

Size (nm)	7,979	12,012	2,939	4,896	6,992	6,648	9,938
ε (%)	0,037	0,029	0,036	0,028	0,029	0,032	0,034
σ(Gpa)	-8,609	-6,776	-8,459	-6,605	-6,741	-7,498	-7,964
δ(nm^{-2})	0,016	0,007	0,116	0,042	0,020	0,023	0,0101

Furthermore, the dislocation parameter (δ), which depends on the broadening of the diffraction peaks as atoms within the crystal unit cell are displaced from their ideal positions, has an average value ranging from 0.007 nm^{-2} to 0.042 nm^{-2}. Dislocation is a defect within the crystal structure that occurs when the atomic arrangement within the crystal experiences shifts or deformations. The data shows that the dislocation density decreases from 0.016 nm^{-2} to 0.007 nm^{-2} as the annealing temperature rises from 300°C to 600°C. This occurs because higher annealing temperatures provide more space for atoms to move and shift to create a perfect crystal, reducing dislocation density.

CONCLUSION

In conclusion, the research successfully fabricated ZnO thin films using the Microwave Assisted Spray Pyrolysis method with annealing temperature variations. The characterization results indicate that annealing temperature significantly influences the properties of ZnO thin films. The optimal annealing temperature is observed at 400°C, where the thin films have fewer defects and cracks. The EDX results show that the Zn percentage in the thin film increases with annealing temperature, reaching its peak at 500°C and then decreasing. The highest Zn percentage is achieved at 500°C, with a value of 78.93%. Regarding the optical properties, the absorbance, transmittance, and bandgap results show that the optimal annealing temperature is 450°C, with the minimum absorbance occurring at wavelengths above 400 nm (visible light), maximum transmittance at 90.77%, and a minimum bandgap value of 3.00 eV. The crystallinity results reveal that the best annealing temperature is between 400°C and 500°C, as indicated by the dominant crystal orientation of (101). All samples are above 50% in crystallinity index, with the best index at 450°C, reaching 81%. These findings suggest that the annealing temperatures from 400°C to 500°C are suitable for TCO applications. The presence of crystal orientations (100), (002), and (101) indicates the potential for solar cell window applications.

REFERENCES

Abidah, N. (2022). *Studi Struktur Dan Sifat Optik Film Tipis Zinx Oxide Doping Ganda Titanium dan Copper Dengan Metode Spin Coating*.

Afre, R. A., Sharma, N., Sharon, M., & Sharon, M. (2018). Transparent conducting oxide films for various applications: A review. *Reviews on Advanced Materials Science*, *53*(1), 79–89. https://doi.org/10.1515/rams-2018-0006

Anitha, M., Saravanakumar, K., Anitha, N., Kulandaisamy, I., & Amalraj, L. (2019). Influence of annealing temperature on physical properties of Sn-doped CdO thin films by nebulized spray pyrolysis technique. *Materials Science and Engineering B: Solid-State Materials for Advanced Technology*, *243*(April 2018), 54–64. https://doi.org/10.1016/j.mseb.2019.03.018

Aryanto, D., Hastuti, E., Taspika, M., Anam, K., Isnaeni, I., Widayatno, W. B., Wismogroho, A. S., Marwoto, P., Nuryadin, B. W., Noviyanto, A., & Sugianto, S. (2020). Characteristics and photocatalytic activity of highly c-axis-oriented ZnO thin films. *Journal of Sol-Gel Science and Technology*, *96*(1), 226–235. https://doi.org/10.1007/s10971-020-05361-5

Ashok, A., Regmi, G., Romero-Núñez, A., Solis-López, M., Velumani, S., & Castaneda, H. (2020). Comparative studies of CdS thin films by chemical bath deposition techniques as a buffer layer for solar cell applications. *Journal of Materials Science: Materials in Electronics*, *31*(10), 7499–7518. https://doi.org/10.1007/s10854-020-03024-3

Astuti, B., Zhafirah, A., Carieta, V. A., Hamid, N., Marwoto, P., Sugianto, Nurbaiti, U., Ratnasari, F. D., Putra, N. M. D., & Aryanto, D. (2020). X-ray diffraction studies of ZnO:Cu thin films prepared using sol-gel method. *Journal of Physics: Conference Series*, *1567*(2). https://doi.org/10.1088/1742-6596/1567/2/022004

Celarel, A., Tuta, C., & Ioan, G. V. (2018). Study of the optical band gap energy associated to optical materials exposed to low doses of gamma-rays. *Romanian Journal of Physics*, *63*(9–10).

Chaitra, U., Kekuda, D., & Mohan Rao, K. (2017). Effect of annealing temperature on the evolution of structural, microstructural, and optical properties of spin coated ZnO thin films. *Ceramics International*, *43*(9), 7115–7122. https://doi.org/10.1016/j.ceramint.2017.02.144

Darsono, T., Muqoyyanah, M., Sulhadi, S., Wahyuni, S., Marwoto, P., & Sugianto, S. (2021). Effect of Post-Annealing Treatment on the Morphological and Optical Properties of ZnO Thin Film Fabricated by Spraying Deposition Method. *Indonesian Journal of Applied Physics*, *11*(1), 113. https://doi.org/10.13057/ijap.v11i1.46927

Espitia, P. J. P., Otoni, C. G., & Soares, N. F. F. (2016). Zinc Oxide Nanoparticles for Food Packaging Applications. In *Antimicrobial Food Packaging*. Elsevier Inc. https://doi.org/10.1016/B978-0-12-800723-5.00034-6

Gadallah, A. S., & El-Nahass, M. M. (2013). Structural, optical constants and photoluminescence of ZnO thin films grown by sol-gel spin coating. *Advances in Condensed Matter Physics*, *2013*. https://doi.org/10.1155/2013/234546

Hadi, S., Marwoto, P., Made, N., Fisika, D. P. J., Matematika, F., Ilmu, D., & Alam, P. (2013). Unnes Physics Journal Deposisi Dan Karakterisasi Film Tipis Cds/Cdte:Cu Yang Ditumbuhkan Dengan Metode Dc Magnetron Sputtering. *Upj*, *2*(1), 44–50. http://journal.unnes.ac.id/sju/index.php/upj

Hardani, H., Hendra, H., Darmawan, M. I., Cari, C., & Supriyanto, A. (2016). Pengaruh Konsentrasi Ruthenium (N719) sebagai Fotosensitizer dalam Dye-Sensitized Solar Cells (DSSC) Transparan. *Jurnal Fisika Dan Aplikasinya*, *12*(3), 104. https://doi.org/10.12962/j24604682.v12i3.1340

Iwantono, I., Anggelina, F., Nurrahmawati, P., Naumar, F. Y., & Umar, A. A. (2016). Optimalisasi Efisiensi Dye Sensitized Solar Cells Dengan Penambahan Doping Logam Aluminium Pada Material Aktif Nanorod Zno Menggunakan Metode Hidrotermal. *Jurnal Material Dan Energi Indonesia*, *06*(01), 36–43.

Jun, M. C., Park, S. U., & Koh, J. H. (2012). Comparative studies of Al-doped ZnO and Gadoped ZnO transparent conducting oxide thin films. *Nanoscale Research Letters*, *7*, 1–6. https://doi.org/10.1186/1556-276X-7-639

Kasirajan, K., Radhi Devi, K., Rajini, M., & Karunakaran, M. (2022). Structural, Morphological and Optical Properties of Perfume Atomizer Spray Pyrolysis CdO Thin Films: Effect of Solution Volume. *Recent Perspectives in Pyrolysis Research*, 1–14. https://doi.org/10.5772/intechopen.99906

Kurtaran, S. (2021). Al doped ZnO thin films obtained by spray pyrolysis technique: Influence of different annealing time. *Optical Materials*, *114*(February), 20–25. https://doi.org/10.1016/j.optmat.2021.110908

Lim, W. Q., Sim, L. K., Fazrina, N., & Maryam, W. (2017). Effect of post annealing temperature on photonic bandgap of ZnO nanorods grown by chemical bath deposition. *AIP Conference Proceedings*, *1838*, 10–15. https://doi.org/10.1063/1.4982174

Lin, K. H., Enomae, T., & Chang, F. C. (2019). Cellulose Nanocrystal Isolation from Hardwood Pulp using Various Hydrolysis Conditions. *Molecules*, *24*(20), 3–5. https://doi.org/10.3390/molecules24203724

López-Suárez, A., Acosta, D., Magaña, C., & Hernández, F. (2020). Optical, structural and electrical properties of ZnO thin films doped with Mn. *Journal of Materials Science: Materials in Electronics*, *31*(10), 7389–7397. https://doi.org/10.1007/s10854-019-02830-8

Loureiro, J., Neves, N., Barros, R., Mateus, T., Santos, R., Filonovich, S., Reparaz, S., Sotomayor-Torres, C. M., Wyczisk, F., Divay, L., Martins, R., & Ferreira, I. (2014). Transparent aluminium zinc oxide thin films with enhanced thermoelectric properties. *Journal of Materials Chemistry A*, *2*(18), 6649–6655. https://doi.org/10.1039/c3ta15052f

Mahmudah, S. N. (2016). Pengaruh Tekanan Oksigen pada Proses Annealing Film Tipis Zinc Oksida (ZnO) Doping Aluminium (Al). In *Universitas Negeri Semarang*. Universitas Negeri Semarang.

Marwoto, P., Khanifah, L., Sulhadi, Sugianto, Astuti, B., & Wibowo, E. (2019). Influence of annealing time on the morphology and oxygen content of ZnO:Ga thin films. *Journal of Physics: Conference Series*, *1321*(2). https://doi.org/10.1088/1742-6596/1321/2/022020

Mehmood, B., Khan, M. I., Iqbal, M., Mahmood, A., & Al-Masry, W. (2021). Structural and optical properties of Ti and Cu co-doped ZnO thin films for photovoltaic applications of dye sensitized solar cells. *International Journal of Energy Research*, *45*(2), 2445–2459. https://doi.org/10.1002/er.5939

Muchuweni, E., Sathiaraj, T. S., & Nyakotyo, H. (2016). Effect of gallium doping on the structural, optical and electrical properties of zinc oxide thin films prepared by spray pyrolysis. *Ceramics International*, *42*(8), 10066–10070. https://doi.org/10.1016/j.ceramint.2016.03.110

Nafisah, H. C. (2022). *Pengembangan Sistem Microwave Assisted Spray Pyrolisis Deposition Untuk Deposisi Material Film Tipis Zinc Oxide*. Universitas Negeri Semarang.

Ponja, S. D., Sathasivam, S., Parkin, I. P., & Carmalt, C. J. (2020). Highly conductive and transparent gallium doped zinc oxide thin films via chemical vapor deposition. *Scientific Reports*, *10*(1), 1–7. https://doi.org/10.1038/s41598-020-57532-7

Rashid, A. R. A., Hazwani, T. N., Mukhtar, W. M., & Taib, N. A. M. (2018). Influence of annealing temperature on optical properties of Al doped ZnO nanoparticles via sol-gel methods. *AIP Conference Proceedings*, *1972*(June). https://doi.org/10.1063/1.5041227

Reeja-Jayan, B., Harrison, K. L., Yang, K., Wang, C. L., Yilmaz, A. E., & Manthiram, A. (2012). Microwave-assisted low-temperature growth of thin films in solution. *Scientific Reports*, *2*, 1–8. https://doi.org/10.1038/srep01003

Rinaldi, R., Amri, A., Jurusan Teknik Kimia, M., & Jurusan Teknik Kimia, D. (2016). Sintesa Fluorinated Tin Oxide (FTO) Menggunakan Prekursor Ramah Lingkungan dan Penambahan Graphene dengan Metode Deposisi Spray Coating Untuk Aplikasi Material Konduktif Transparan. In *Jom FTEKNIK*.

Rustandi, A., Anrokhi, M. S., Nuryantini, A. Y., Iskandar, F., Abdullah, M., & Khairurrijal. (2012). *Sintesis Komposit Nanokristalin α -Fe 2 O 3 / Zeolit Alam Dengan Metode Spray Pyrolysis*. 3–6.

Saha, J. K., Bukke, R. N., Mude, N. N., & Jang, J. (2020). Significant improvement of spray pyrolyzed ZnO thin film by precursor optimization for high mobility thin film transistors. *Scientific Reports*, *10*(1), 1–11. https://doi.org/10.1038/s41598-020-65938-6

Samad, N. A. A., Lai, C. W., & Johan, M. R. (2020). Chemical studies of metal oxide powders. In *Metal Oxide Powder Technologies*. INC. https://doi.org/10.1016/b978-0-12-817505-7.00002-6

Sinaga, P. (2015). Pengaruh Temperatur Annealing Terhadap Struktur Mikro, Sifat Listrik Dan Sifat Optik Dari Film Tipis Oksida Konduktif Transparan Zno:Al Yang Dibuat Dengan Teknik Screen Printing. *Jurnal Pengajaran Matematika Dan Ilmu Pengetahuan Alam*, *14*(2), 1–9. https://doi.org/10.18269/jpmipa.v14i2.301

Sugianto, Zannah, R., Mahmudah, S., Astuti, B., Putra, N., Wibowo, A., Marwoto, P., Ariyanto, D., & Wibowo, E. (2016). Pengaruh Temperatur Annealing Pada Sifat Listrik Film Tipis Zinc Oksida Doping Aluminium Oksida. *Jurnal MIPA*, *39*(2), 115–122. http://journal.unnes.ac.id/nju/index.php/JM

Sulhadi, Fatiatun, Marwoto, P., Sugianto, & Wibowo, E. (2015). Variasi suhu Deposisi paDa struktur, sifat optik Dan Listrik fiLm tipis seng oksiDa Dengan Doping gaLium (Zno:ga). *Jurnal Pendidikan Fisika Indonesia*, *11*(1), 93–99. https://doi.org/10.15294/jpfi.v11i1.4007

Sulhadi, Muqoyyanah, Darsono, T., Wahyuni, S., Sugianto, & Marwoto, P. (2021). Optical properties of zinc oxide thin film fabricated by spraying deposition method. *Journal of Physics: Conference Series*, *1918*(2), 8–12. https://doi.org/10.1088/1742-6596/1918/2/022002

Tian, T., Cheng, L., Zheng, L., Xing, J., Gu, H., Bernik, S., Zeng, H., Ruan, W., Zhao, K., & Li, G. (2016). Defect engineering for a markedly increased electrical conductivity and power factor in doped ZnO ceramic. *Acta Materialia*, *119*, 136–144. https://doi.org/10.1016/j.actamat.2016.08.026

Vittal, R., & Ho, K. C. (2017). Zinc oxide based dye-sensitized solar cells: A review. *Renewable and Sustainable Energy Reviews*, *70*(December 2016), 920–935. https://doi.org/10.1016/j.rser.2016.11.273

Wang, Z. B., Helander, M. G., & Lu, Z. H. (2013). Transparent conducting thin films for OLEDs. *Organic Light-Emitting Diodes (OLEDs): Materials, Devices and Applications*, 49–76. https://doi.org/10.1533/9780857098948.1.49

Wypych, G. (2015). Principles of Uv Degradation. *PVC Degradation and Stabilization*, 167–203. https://doi.org/10.1016/b978-1-895198-85-0.50007-8

Yousaf, S., Ahmad, I., Kanwal, M., Alshahrani, T., Alhashim, H. H., Kattan, N. A., Tahir Farid, H. M., Riaz, A., Mehran, T., & Laref, A. (2021). Structural and electrical properties of Ba-substituted spinel ferrites. *Materials Science in Semiconductor Processing*, *122*(September 2020), 105488. https://doi.org/10.1016/j.mssp.2020.105488

Zhang, L., Lan, J., Yang, J., Guo, S., Peng, J., Zhang, L., Tian, S., Ju, S., & Xie, W. (2017). Study on the physical properties of indium tin oxide thin films deposited by microwave-assisted spray pyrolysis. *Journal of Alloys and Compounds*, *728*, 1338–1345. https://doi.org/10.1016/j.jallcom.2017.09.024

Zheng, Q., Li, Z., Yang, J., & Kim, J. K. (2014). Graphene oxide-based transparent conductive films. *Progress in Materials Science*, *64*, 200–247. https://doi.org/10.1016/j.pmatsci.2014.03.004

Zhou, N., Buchholz, D. B., Zhu, G., Yu, X., Lin, H., Facchetti, A., Marks, T. J., & Chang, R. P. H. (2014). *Ultrafl exible Polymer Solar Cells Using Amorphous Zinc − Indium − Tin Oxide Transparent Electrodes*. 1098–1104. https://doi.org/10.1002/adma.201302303